Hindawi Publishing Corporation
Journal of Nanomaterials
Volume 2015, Article ID 747420, 11 pages
http://dx.doi.org/10.1155/2015/747420

Research Article

Effects of Chitosan Concentration on the Protein Release Behaviour of Electrospun Poly(ε-caprolactone)/Chitosan Nanofibers

Fatemeh Roozbahani,[1] Naznin Sultana,[1] Davood Almasi,[2] and Farnaz Naghizadeh[1]

[1]*Faculty of Biosciences and Medical Engineering, Universiti Teknologi Malaysia, UTM Skudai, 81310 Johor Bahru, Johor, Malaysia*
[2]*Department of Manufacturing and Industrial Engineering, Faculty of Mechanical Engineering, Universiti Teknologi Malaysia, 81310 Johor Bahru, Johor, Malaysia*

Correspondence should be addressed to Naznin Sultana; naznin@biomedical.utm.my

Received 15 October 2014; Accepted 6 December 2014

Academic Editor: Naeem Faraz

Poly(ε-caprolactone)/chitosan (PCL/chitosan) blend nanofibers with different ratios of chitosan were electrospun from a formic acid/acetic acid (FA/AA) solvent system. Bovine serum albumin (BSA) was used as a model protein to incorporate biochemical cues into the nanofibrous scaffolds. The morphological characteristics of PCL/chitosan and PCL/chitosan/BSA Nanofibers were investigated by scanning electron microscopy (SEM). Fourier transform infrared spectroscopy (FTIR) was used to detect the presence of polymeric ingredients and BSA in the Nanofibers. The effects of the polymer blend ratio and BSA concentration on the morphological characteristics and consequently on the BSA release pattern were evaluated. The average fiber diameter and pore size were greater in Nanofibers containing BSA. The chitosan ratio played a significant role in the BSA release profile from the PCL/chitosan/BSA blend. Nanofibrous scaffolds with higher chitosan ratios exhibited less intense bursts in the BSA release profile.

1. Introduction

Tissue engineering scaffolds in the form of electrospun nanofibers provide support for cells to adhere, grow, and propagate by mimicking the natural extracellular matrix (ECM) structure [1]. Nanofibers have the following several advantages as tissue engineering scaffolds: (i) a high surface area for the delivery of drugs, nutrients, and biochemical materials through the seeded cells; (ii) a structure comprised of a network of interconnected pores; (iii) high porosity for cells to migrate and nutrients and metabolic waste to flow in vivo.

In addition to architecture, biomolecules are another vital element for cell attachment, proliferation, and differentiation and should be released in a constant and controlled manner, maintaining their bioactivity. Therefore, the aforementioned morphological characteristics coupled with controlled biomolecule delivery provide both morphological and biomedical applications for tissue regeneration. Nonetheless, research in this area is still quite limited [2–12], although the release pattern of pharmaceutical drugs with nanofibrous scaffolds has already been considered by a number of authors [13–19].

Blend [3], emulsion [5, 10, 20], and coaxial [3, 9, 12] electrospinning are three conventional electrospinning techniques for the incorporation of biomolecules into fibers. Researchers have reported burst release as a disadvantage of blend electrospinning comparing with coaxial electrospinning, which requires a special apparatus and careful selection of materials. Emulsion electrospinning has attracted increasing attention in recent years due to its simplicity [7]. Nevertheless, the effects of emulsifiers as an additive in electrospinning are still unknown. Generally, the compatibility of the polymer, drug, and other ingredients affects the release profile [21].

Chitosan is a partially deacetylated derivative of chitin, the second most abundant polysaccharide in nature [22]. It has several unique characteristics that are beneficial for

biomedical applications, such as its biodegradable, biocompatible, nontoxic, and antibacterial properties. The electrospinning of pure chitosan and its blends with synthetic polymers, proteins, and inorganic nanoparticles has been studied [23, 24]. Chitosan is soluble in most organic acids. The electrospinning of chitosan is relatively complicated due to its high molecular weight, high viscosity, and high density of positive charges in acidic solution [25–28]. The electrospinning of chitosan in a blend with a second polymer with a flexible structure and lower molecular weight is a potential solution to this problem. In further attempts to minimise the limitation of molecular weight on the electrospinning process, even in blends with a second polymer, reducing the molecular weight of chitosan through alkali treatment has been investigated [29, 30].

Poly ε-caprolactone (PCL) has been used for scaffold fabrication and the controlled release of drugs and biomolecules [31–33], but it has several drawbacks, such as its hydrophobicity, initial burst release, and extremely long degradation period. To overcome the abovementioned drawbacks, blends of PCL and other natural or synthetic polymers, such as gelatin and chitosan, have been used [31, 33–35]. Studies related to nanofibrous scaffolds composed of PCL/chitosan blends are very rare due to their lack of common solvent systems.

In 2012 [36] introduced a solution system consisting of formic acid/acetic acid (FA/AA) as a substitute for previous expensive and toxic solvents [32, 33, 37]. This new solvent system opens the door for further feasibility studies for PCL/chitosan scaffolds as means to simulate the basic requirements of ECM. Bovine serum albumin (BSA) as a model protein was added to the solvent system to generate biochemical signals in fabricated scaffolds.

The aim of this study was to fabricate PCL/chitosan nanofibrous scaffolds with BSA from FA/AA solution via blend electrospinning. Nanofibers with different PCL/chitosan/BSA ratios have been fabricated and investigated in terms of fiber diameter, pore size, and BSA release behaviour. The main objective was to show that the BSA release profile could be finely tailored by modulation of the morphology, porosity, and composition of the nanofibers. The results illustrated that the morphological characteristics play a fundamental rule in explaining the release pattern of nanofibers.

2. Materials and Methods

2.1. Materials. Medium-molecular-weight chitosan, poly(ε-caprolactone) (PCL), bovine serum albumin (BSA), and phosphate-buffered saline (PBS) all were obtained from Sigma-Aldrich for use in the protein release studies. The solvents, including formic acid (FA; 98%) and acetic acid (AA; 99.8%), were supplied by Merck.

2.2. Electrospinning. The electrospinning solutions were prepared by simultaneously adding certain amounts of PCL and chitosan to a mixed solvent system and stirring for 3 h. The solvent system was composed of formic acid/acetic acid (FA/AA) in a ratio of 70/30 [36, 38].

The PCL and chitosan concentrations were expressed in wt.% relative to the solution, while the BSA concentration was presented as the wt.% relative to the total polymeric material (PCL and chitosan).

To prepare electrospun nanofibers, approximately 2 mL of the prepared solution was placed in a 5 mL syringe. A 23-gauge needle was used for the spinning process. The distance from the needle to the collector was fixed at 12.5 cm, and the voltage range of stable electrospinning was generally in the range of 18 to 25 kV depending on the stability of the Taylor cone during the process. Electrospinning was carried out at room temperature (22 ± 2°C) and a relative humidity of 65 ± 5%. The flow rate was set at 0.5 mL h^{-1}.

2.3. Protein Loading in the Electrospun Scaffolds. Protein was loaded on the nanofibers using the blend electrospinning technique. First, solutions of 8 wt.% PCL and different concentrations of chitosan (0.2, 0.4, 0.6, 0.8, and 1 wt.%) were prepared. Next, 5, 10, 15, and 20% BSA were added to the solution systems to determine the optimum BSA concentration in terms of fiber morphology and protein release behaviour. Lastly, the experiments for preliminary solvents were repeated with the optimum amount of BSA.

2.4. Characterisation of Electrospun Scaffolds

2.4.1. Scanning Electron Microscopy (SEM). To evaluate the morphology of the electrospun scaffolds, electrospun nanofibrous samples were cut into small pieces, sputter-coated with gold, and imaged using a Hitachi TM-3000 SEM apparatus. The fiber diameters and pore sizes of the scaffolds were analysed using image visualisation software (ImageJ, National Institute of Health, Bethesda, MD; http://rsb.info.nih.gov/ij/). Approximately 100 counts per image were used to calculate the fiber diameter.

2.4.2. Pore Size. As a morphological characteristic of nanofibrous matrices, the pore size of the electrospun PCL/chitosan was measured. To this end, nanofibers were electrospun for 5 min for each blend. The surface porosity of the electrospun web was calculated by processing the SEM images and measuring the free space between nanofibers, which corresponds to the dark area in the SEM images.

2.4.3. FTIR. FTIR spectroscopy was used to identify the components in the blend and the changes to the blend composition after adding BSA. Samples of the same dimensions were mixed with potassium bromide to form pellets. FTIR spectra in transmission mode were recorded using an FTIR spectrometer (Perkin Elmer, USA) connected to a PC, and the data were analysed using IR Solution software.

2.5. In Vitro Protein Release Study. For the in vitro release studies, all nanofibrous membranes were cut into small squares (1 × 1 cm^2) and then immersed in 2 mL microtubes containing PBS (pH = 7.4) at 37°C. After predetermined intervals of time, the release buffer was completely replaced with fresh PBS and placed in a water bath to continue

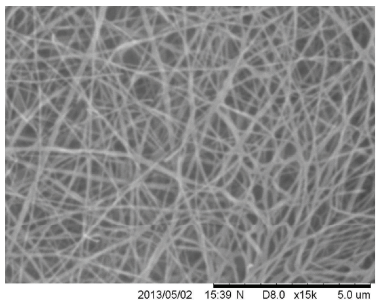

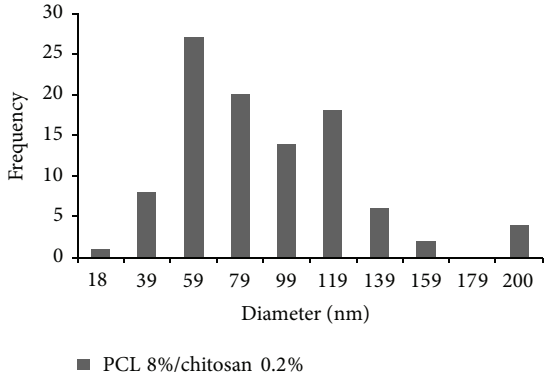

(a)

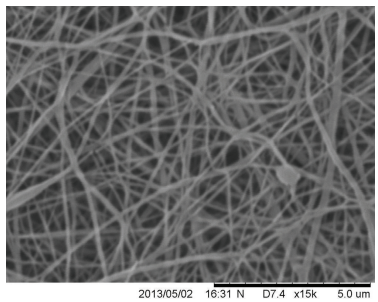

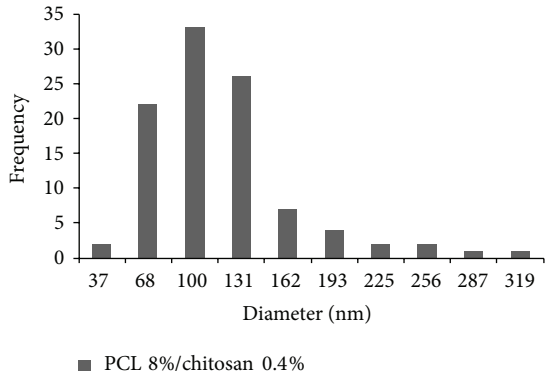

(b)

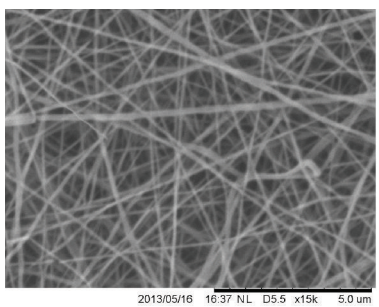

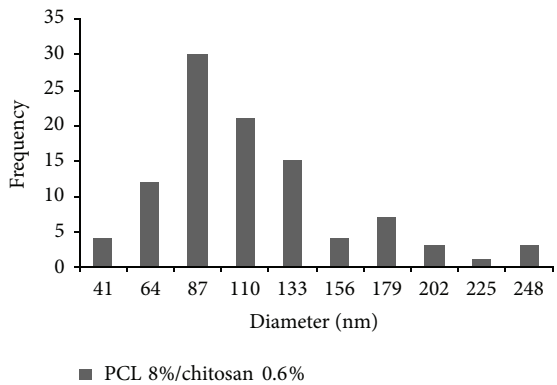

(c)

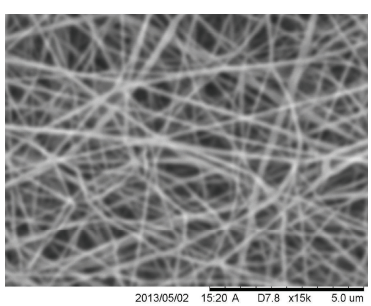

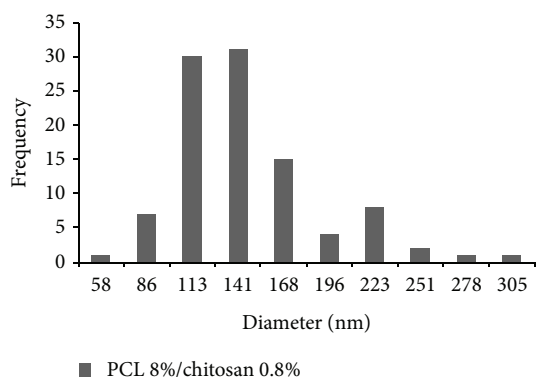

(d)

Figure 1: Continued.

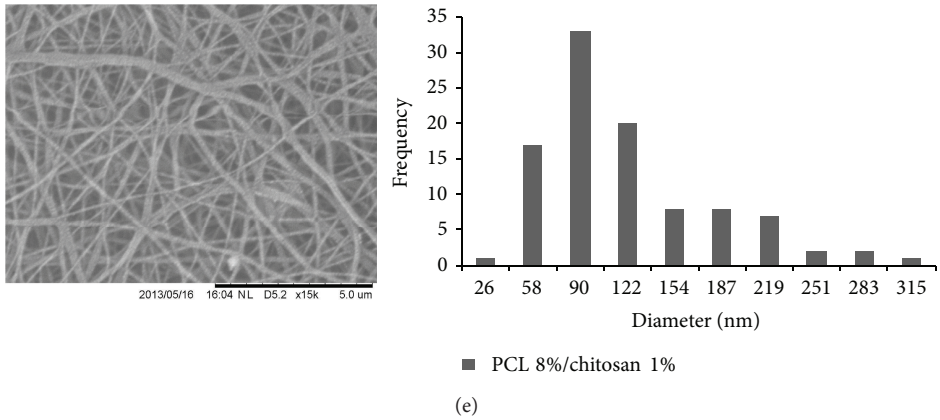

Figure 1: SEM images of PCL/chitosan nanofibers with wt.% ratio of (a) 8/0.2, (b) 8/0.4, (c) 8/0.6, (d) 8/0.8, and (e) 8/1 with fiber diameter frequency diagrams.

the release study. The concentration of each retrieved BSA solution was then determined by measuring the absorbance at 280 nm using a UV-Vis spectrophotometer (Hitachi Corp., Tokyo, Japan). The concentrations were calculated using the Beer-Lambert law:

$$A = \varepsilon bc, \tag{1}$$

where A is the absorbance, b is the path length of the sample, that is, the path length (cm) of the cuvette in which the sample is contained, ε is the molar absorptivity with units of $\mathrm{L\,mol^{-1}\,cm^{-1}}$, and c is the concentration of the compound in solution, expressed in $\mathrm{mol\,L^{-1}}$.

The results were demonstrated in terms of cumulative amount released (%):

$$\text{Cumulative release}\,\% = \left(\frac{M_t}{M_\infty}\right) \times 100, \tag{2}$$

where M_t is the amount of BSA at time t and M_∞ is the total amount of BSA in the nanofibrous membrane.

After completing the release study, the samples were dried using tissue paper, and each sample was dissolved in 3 mL of methylene chloride. The amount of protein extracted was assayed in a similar manner as described above.

3. Results and Discussion

3.1. Morphology. Figure 1 shows the SEM micrographs of the PCL/chitosan fibrous material made with 8 wt.% PCL and chitosan concentrations ranging from 0.2 to 1 wt.% without protein encapsulation, which was fabricated under the conditions described in Section 2.2. The fiber diameter distribution was presented for all samples. The mean diameter of the PCL/chitosan fibers increased gradually from 82.39 to 131.85 nm with the chitosan ratio in the blend (Table 1(a)), except for the last chitosan ratio, which produced a narrower fiber with a ribbon-like structure. For lower chitosan ratios (Figures 1(a) and 1(b)), the nanofibrous structure displayed beads alongside the nanofibers.

The stable electrospinning of pure PCL in FA/AA as a solvent system was only possible at relatively high concentrations, starting from 12 wt.% [38]. Below this concentration, the electrospun nanofibers most resembled a string of beads, and the process condition was not stable regarding the formation of the Taylor cone. Chitosan, even when added in smaller quantities, increased the solution viscosity sufficiently for the spinning process to be possible with a mix of PCL/chitosan at a lower wt.% of PCL [36, 38].

The pore size increased with increasing chitosan concentration, except for the highest concentration, at which the pore size decreased from 421.61 nm for 0.8 wt.% chitosan to 335.61 nm for 1 wt.% chitosan (Table 1(b)). Increasing the solid material content produced a more viscous solution, which, along with aggregation of the positive charges of chitosan in the acidic solvent in the needle, affected the morphological properties of the polymer in the distance between the syringe and the collector such that a higher repulsive force on the polymer string was required to leave the needle. Thus, a smaller fiber diameter and larger pore size resulted.

The impact of the BSA concentration on the PCL/chitosan nanofiber morphology is illustrated in Figure 2. To study the effects of BSA concentration on electrospun nanofibers, different amounts of BSA (5%, 10%, 15%, and 20%) were added to 8% PCL and 0.6% chitosan. The polymer jet containing BSA carries extra charges, which induce a more effective elongation and finer fibers at the same applied voltage. Nevertheless, as the BSA concentration increased, the average fiber diameter increased due to the presence of more solid material in the solvent system [7]. The results showed no significant changes in the mean fiber diameter, except for an increase at 10% BSA, which was approximately 10 nm and was negligible under these criteria. The fiber diameter fluctuated slightly from 122.4 nm for 5% BSA to 109.95 nm for 20% BSA, whereas the pore size increased from 387.19 to 490.24 nm (Table 2). The fiber diameter initially increased gradually due to the naturalisation effect of the functional groups of BSA molecules on the positive charges of chitosan.

Table 1: (a) Fiber diameter and (b) pore size calculated for PCL/chitosan nanofibers comparing PCL/chitosan/BSA nanofibers.

(a)

PCL/chitosan wt.% ratio	Average fiber diameter (nm)	Coefficient of deviation (%)	Average fiber diameter (nm)	Coefficient of deviation (%)
	Without BSA		With 20 wt.% BSA	
8/0.2	82.39	3.73	108.68	5.72
8/0.4	101.69	4.93	123.58	5.37
8/0.6	101.66	4.51	121.54	5.48
8/0.8	131.85	4.45	132.73	5.17
8/1.0	109.01	6.24	159.12	7.66

(b)

PCL/chitosan wt.% ratio	Average pore size (nm)	Coefficient of deviation (%)	Average pore size (nm)	Coefficient of deviation (%)
	Without BSA		With 20% BSA	
8/0.2	233.62	11.63	462.89	24.97
8/0.4	322.96	12.64	437.28	18.57
8/0.6	423.56	21.42	554.14	34.06
8/0.8	421.61	22.05	621.52	35.79
8/1.0	335.61	19.02	783.77	41.85

Table 2: Applied voltage and average nanofibers diameter and pore size in electrospinning PCL/chitosan nanofibers with different BSA%.

BSA wt.%	Voltage (KV)	Average fiber diameter (nm)	Coefficient of deviation (%)	Average pore size (nm)	Coefficient of deviation (%)
5	18	122.4	5.60	387.19	21.25
10	21	133.47	5.60	429.45	24.88
15	20	117.39	6.74	418.43	22.71
20	21	109.95	5.09	490.24	25.10

When the BSA concentration was increased to 15% and 20%, the extra charges produced a finer fiber. The increase in pore size is also attributed to greater repellence between the polymer jet after leaving the needle tip and before grounding. The assessment of the effect of the BSA ratio on the nanofibers release property will be considered in Section 3.3.

Adding 20% BSA to all formulations of the PCL/chitosan blend necessitated a 2-3 kV higher voltage for all samples (Figure 2(a)) to achieve the stable conditions for electrospinning.

The SEM images of different formulations of PCL/chitosan with 20% BSA are shown in Figures 3(a)–3(e). The PCL/chitosan nanofibers diameters increased steadily by approximately 23 ± 4 nm in all cases as a result of the addition of BSA. Alternatively, the pore sizes increased by 50% compared to the samples without BSA. This may be related to the repelling effects of the same charges of the BSA molecules, which moved to the surface of the nanofibers during the bending and splaying before collecting on the collector [39].

Comparing Figures 1(a) and 1(b), no beads were formed during the electrospinning. This effect is related to the compensation of the low viscosity by adding BSA to the system. In Figure 3(e), although the solid material was the same as the sample in Figure 1(e) except for the presence of BSA, fine nanofibers were formed, and no ribbon shape was observed. This result can be ascribed to the modifying effect of BSA for chitosan positive charges in the needle and the reduction of the repelling force applied to the polymer during the spinning process.

Figure 4(a) shows the applied voltages for each group of PCL/chitosan with or without BSA. The voltage was adjusted based on the stable Taylor cone during the process. As expected, higher chitosan concentrations required higher voltages for electrospinning, which is related to the higher viscosity of the solution resulting from the increased chitosan concentration.

All of the data related to the mean fiber diameter, average pore size, and coefficient of deviation are summarised in Tables 1(a) and 1(b). Figures 4(b) and 4(c) compare the characteristics of the PCL/chitosan blend nanofibers after inserting BSA. The figures also show that BSA increased the fiber diameter and pore size in all PCL/chitosan blend formulations.

3.2. FTIR. FTIR spectroscopy was performed to detect the polymeric ingredients and BSA in the fabricated nanofibers. The main features of the FTIR spectrum of chitosan powder included the carboxylate band in the range of 1400 to 1790 cm^{-1}, with a maximum at 1675 cm^{-1}, and a N–H band

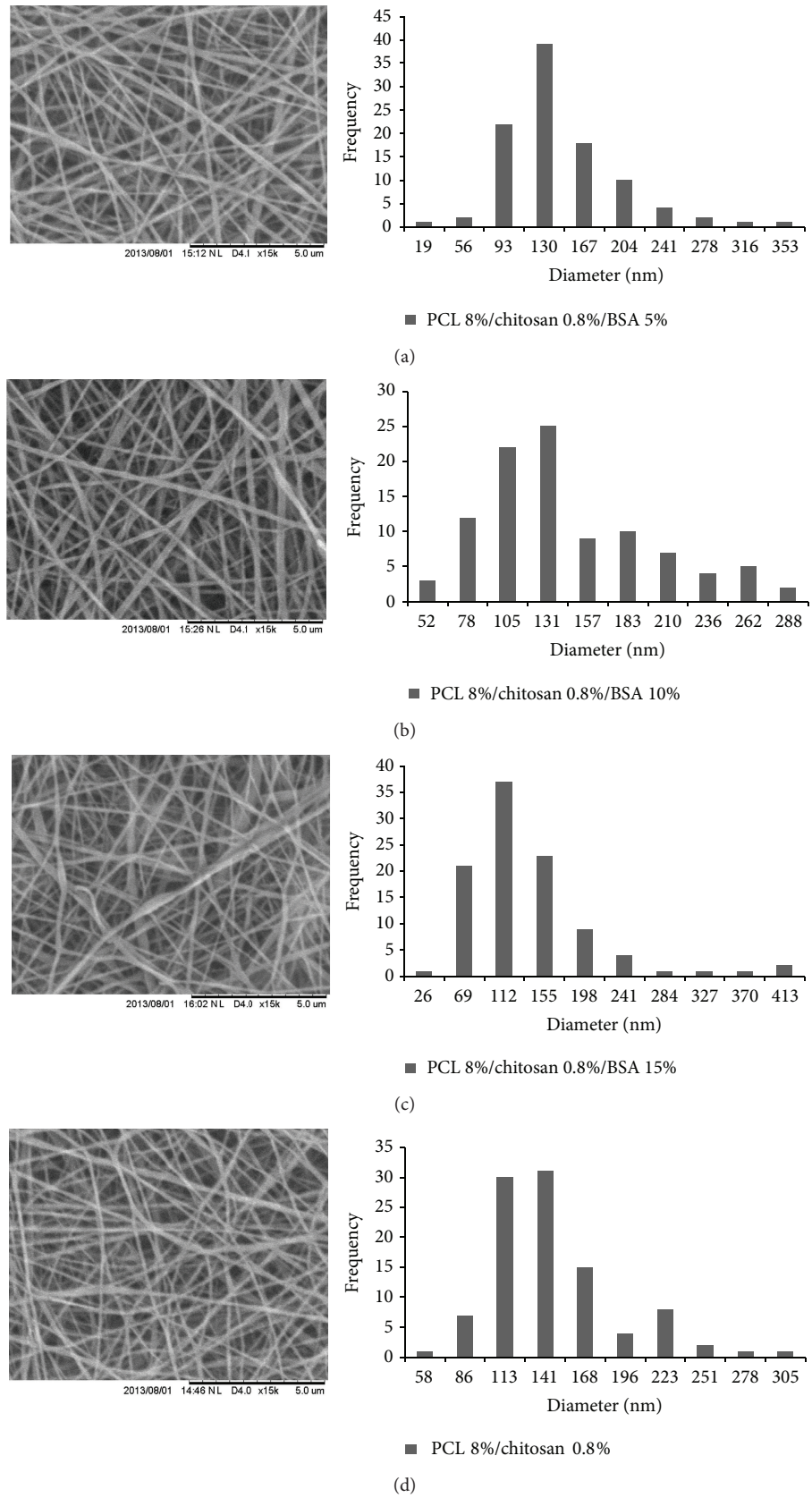

Figure 2: SEM images of PCL/chitosan/BSA nanofibers with BSA different concentration of (a) 5%, (b) 10%, (c) 15%, and (d) 20% with fiber diameter frequency diagrams.

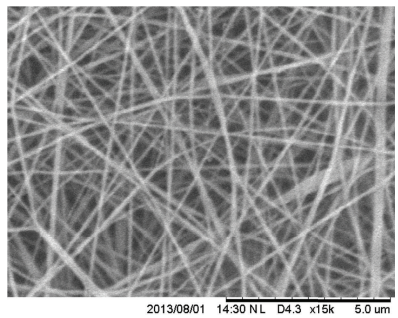

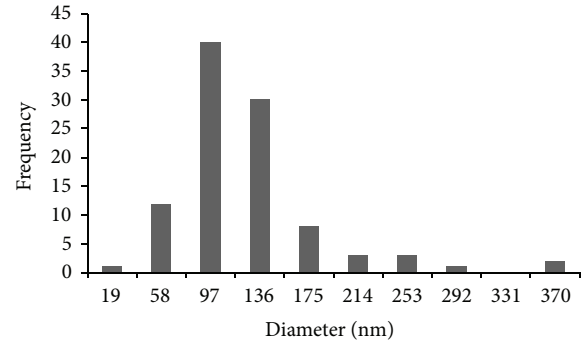

(a)

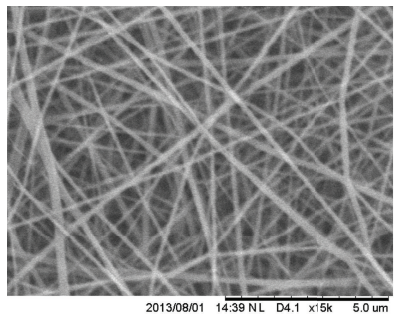

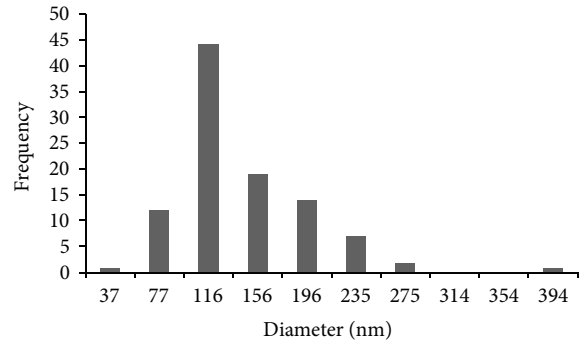

(b)

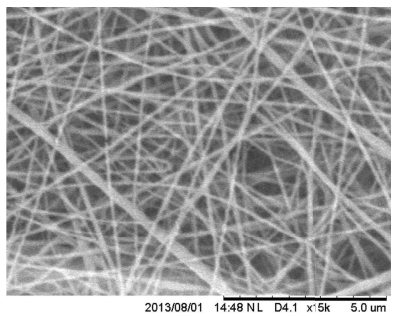

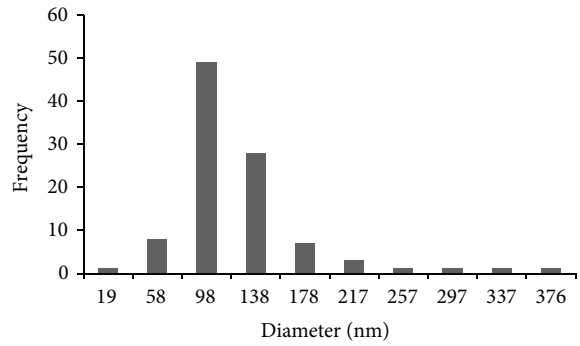

(c)

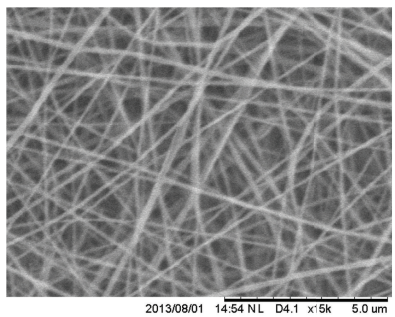

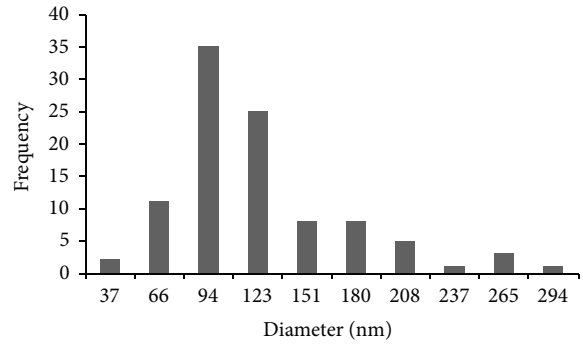

(d)

Figure 3: Continued.

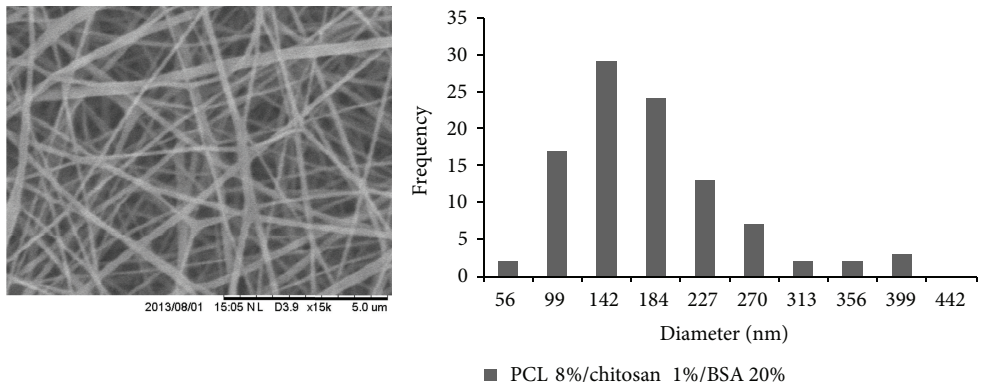

(e)

Figure 3: SEM images of PCL/chitosan/BSA nanofibers with 20% BSA and different PCL/chitosan wt.% ratio of (a) 8/0.2, (b) 8/0.4, (c) 8/0.6, (d) 8/0.8, and (e) 8/1 with fiber diameter frequency diagrams.

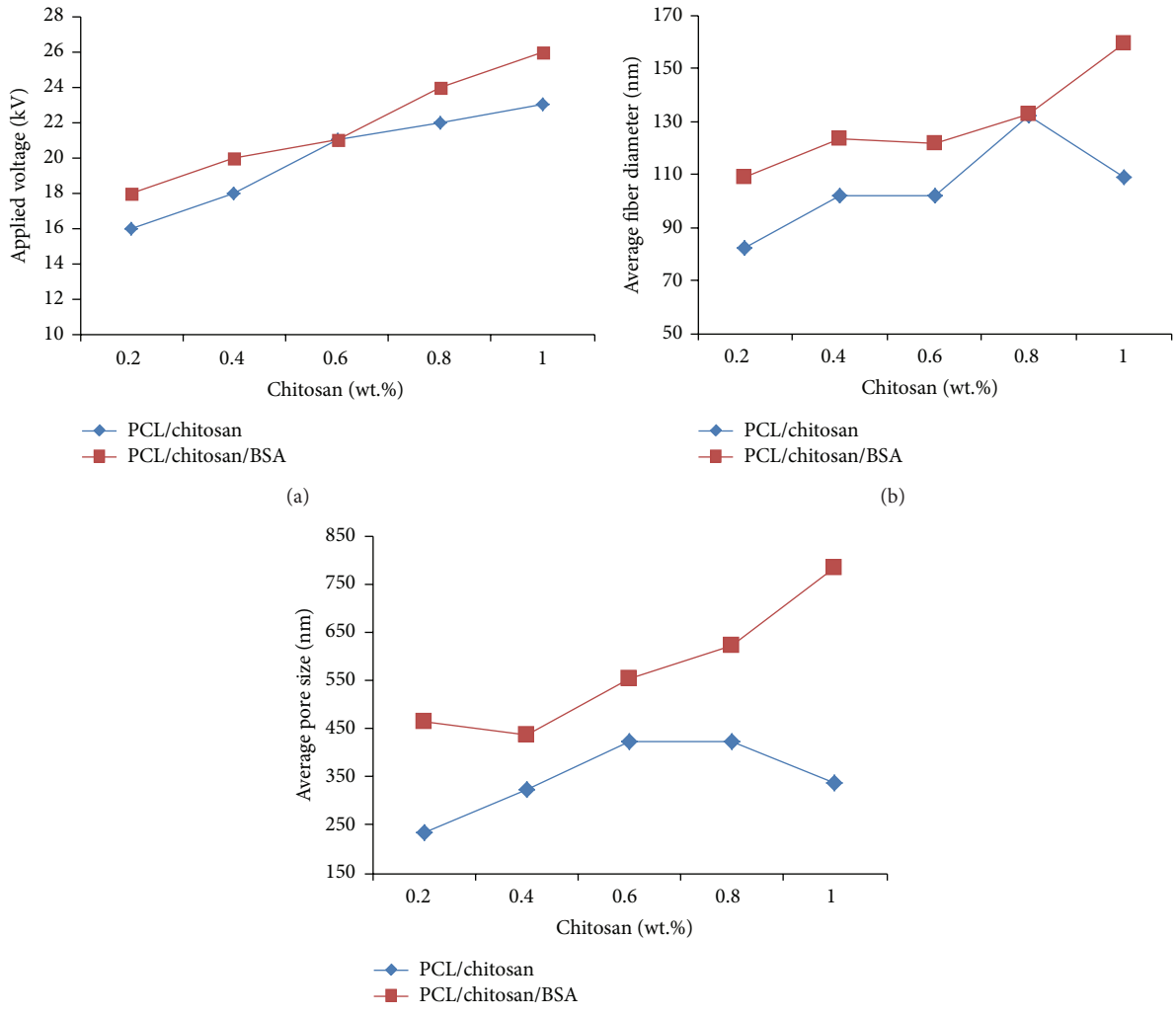

Figure 4: (a) Applied voltage, (b) average nanofibers diameters, and (c) average pore size of PCL/chitosan versus PCL/chitosan BSA nanofibers.

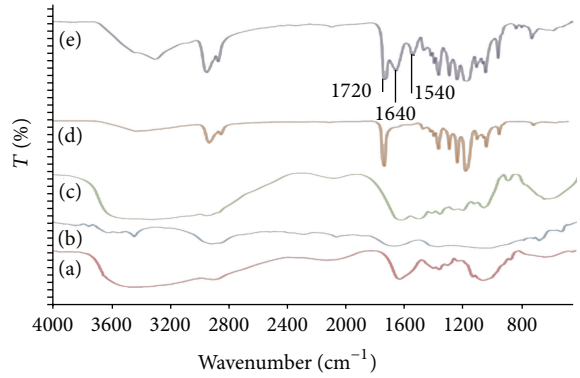

FIGURE 5: FTIR graph: (a) chitosan powder, (b) PCL granule, (c) BSA powder, (d) PCL/chitosan nanofibers, and (e) PCL/chitosan/BSA nanofibers.

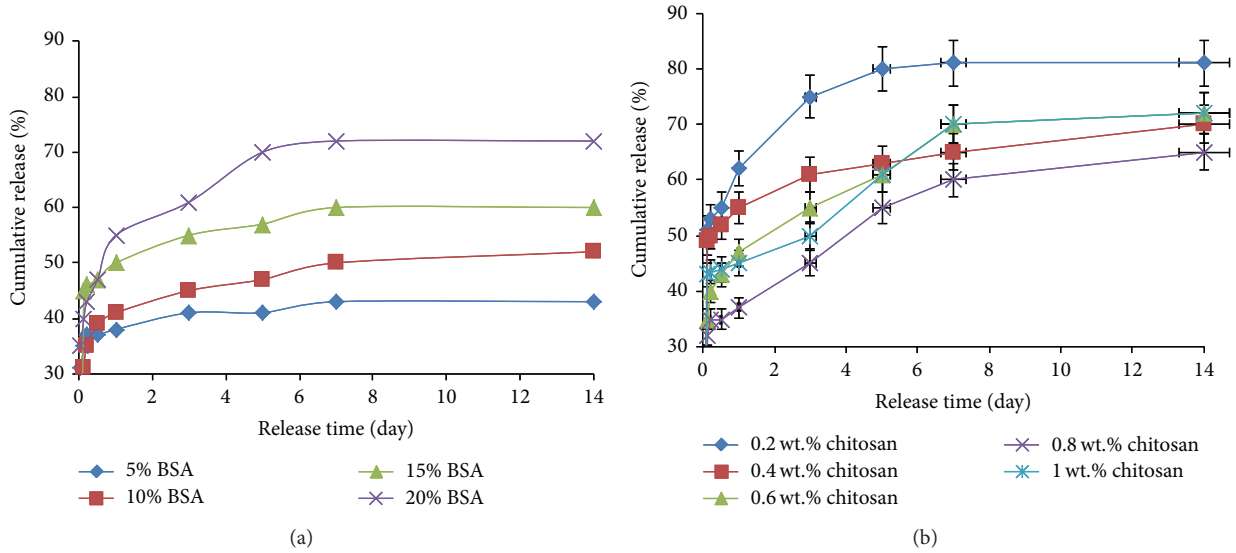

FIGURE 6: Release profile of BSA from PCL/chitosan/BSA blend nanofibers (a) with different BSA and (b) with different PCL/chitosan ratio.

at approximately 3350 cm^{-1} (Figure 5(a)). PCL exhibited a strong absorption at 1720 cm^{-1} corresponding to its carbonyl group (Figure 5(b)). The FTIR spectra in Figure 6(d) included contributions from the carboxylate and amine groups of chitosan and the carbonyl group of PCL. No additional peaks were observed, indicating that the chitosan was embedded physically within the nanofibers.

Figure 5(c) depicts the FTIR spectrum of BSA powder. The main absorption bands of BSA were located at 1640 and 1540 cm^{-1}, which correspond to the protein-related amide I and II absorptions. The spectrum of the PCL/chitosan nanofibers containing BSA (Figure 5(e)) showed both peaks for BSA as well as the characteristic peaks for PCL and chitosan, which confirmed the presence of BSA in the blend nanofibers.

3.3. Release Kinetics. The release profiles of PCL/chitosan/BSA blend nanofibers with different proportions of BSA are shown in Figure 6(a). The release kinetics can be described as consisting of two phases: an initial burst at approximately 30–40% of the total BSA during the first hours of the release study and a gradual release until 14 days, at which point the 80% of the release had been accomplished [40].

During the release experiments, the BSA existing on the surface leaves the nanofibers to enter the release solution. In the case of nanofibers that were electrospun from a mixture of drugs, biomolecules, and polymer, the drugs and/or biomolecules are likely to conglomerate on the surface. Consequently, a poor burst release of the dissolved drug is generally observed in the early phase.

Nanofibers with higher BSA concentration exhibited a more robust burst in the first stage and a longer delay of the second stage than those with lower BSA concentrations. As described in Section 3.1, for equivalent PCL/chitosan, a higher amount of BSA decreased the nanofibers diameter and increased the pore size. Although the changes in the nanofibers diameter were negligible due to the complexity of the interaction between the chitosan and BSA charges, the overall movement of BSA molecules from the nanofibers surface to the release medium was easier for nanofibrous matrices with higher surface areas and larger pore sizes. Additionally, a higher BSA concentration led to greater

uptake on the nanofibers surface and a stronger diffusion force encouraging the molecules to enter the release medium. As shown in Figure 6(a), a higher amount of BSA led to a more intense sustained release stage: 75% for 20% BSA compared to 42% for 5% BSA for blend nanofibers. It was clear that the release was not completed, and the rest of the BSA may continue to release over a longer time period.

The release pattern in PCL/chitosan/BSA nanofibers as a function of chitosan ratio is shown in Figure 6(b). Nanofibers with higher amounts of chitosan demonstrated less intense bursts and more sustained behaviour in the second stage of release. Nanofibers with 0.2 wt.% chitosan had 51% burst in the first hour of the release study, compared to 43% for 1 wt.% chitosan and 35% and 32% for 0.6 and 0.8 wt.% chitosan, respectively. Nanofibrous matrices with 0.8 wt.% chitosan exhibited a release pattern similar to the sustained release kinetics. The deviation of 1 wt.% chitosan from this trend was strongly related to the BSA saturation of its surface.

Based on the morphological studies, nanofibers with higher chitosan content exhibited a higher fiber diameter and pore size. Thus, similar to the aforementioned discussion for nanofibers with different BSA contents, the determined amount of nanofibrous scaffold with higher surface area and larger pore size is correlated with stronger burst release for nanofibers with less chitosan. However, BSA contains more charged groups (such as $-NH_2$ and –COOH) than PCL. Therefore, BSA was forced to move onto the fiber surface by the electric forces during electrospinning and was thereby in strong competition with chitosan. Consequently, chitosan limits BSA transfer to the surface of nanofibers and ultimately decreases the release amount of BSA in release graphs for PCL/chitosan/BSA with higher chitosan contents.

4. Conclusion

BSA as a model protein was successfully embedded in PCL/chitosan blend nanofibers using FA/AA as solvent system through a blending electrospinning technique. Compared to PCL/chitosan nanofibers, PCL/chitosan/BSA nanofibers had higher fiber diameter and larger pore size. Some electrospinning defects, such as beads at lower chitosan concentrations and ribbon-like nanofibers, were observed because of the accumulation of chitosan positive charges in the needle during electrospinning. This phenomenon was reduced by adding BSA. PCL/chitosan/BSA nanofibers with higher chitosan concentrations exhibited less intense bursts in the first hour of BSA release, which was related to the higher diameter and consequently lower surface area of the nanofibers exposed to the release medium.

Conflict of Interests

The authors declare that there is no conflict of interests regarding the publication of this paper.

Acknowledgments

The authors would like to thank Universiti Teknologi Malaysia for the International Doctoral Fellowship. The authors also acknowledge MOHE, GUP Tier 1 grants (Vot: 03H13, Vot: 05H07), FRGS (Vot: 4F126), MOHE, UTM, and RMC for financial support. The lab facilities of FBME are also acknowledged.

References

[1] R. Langer and J. P. Vacanti, "Tissue engineering," *Science*, vol. 260, no. 5110, pp. 920–926, 1993.

[2] S. Y. Chew, J. Wen, E. K. F. Yim, and K. W. Leong, "Sustained release of proteins from electrospun biodegradable fibers," *Biomacromolecules*, vol. 6, no. 4, pp. 2017–2024, 2005.

[3] W. Ji, F. Yang, J. J. J. P. Van Den Beucken et al., "Fibrous scaffolds loaded with protein prepared by blend or coaxial electrospinning," *Acta Biomaterialia*, vol. 6, no. 11, pp. 4199–4207, 2010.

[4] H. Jiang, Y. Hu, Y. Li, P. Zhao, K. Zhu, and W. Chen, "A facile technique to prepare biodegradable coaxial electrospun nanofibers for controlled release of bioactive agents," *Journal of Controlled Release*, vol. 108, no. 2-3, pp. 237–243, 2005.

[5] X. Li, Y. Su, S. Liu, L. Tan, X. Mo, and S. Ramakrishna, "Encapsulation of proteins in poly(L-lactide-co-caprolactone) fibers by emulsion electrospinning," *Colloids and Surfaces B: Biointerfaces*, vol. 75, no. 2, pp. 418–424, 2010.

[6] S. Maretschek, A. Greiner, and T. Kissel, "Electrospun biodegradable nanofiber nonwovens for controlled release of proteins," *Journal of Controlled Release*, vol. 127, no. 2, pp. 180–187, 2008.

[7] M. Norouzi, M. Soleimani, I. Shabani, F. Atyabi, H. H. Ahvaz, and A. Rashidi, "Protein encapsulated in electrospun nanofibrous scaffolds for tissue engineering applications," *Polymer International*, vol. 62, no. 8, pp. 1250–1256, 2013.

[8] C. M. Valmikinathan, S. Defroda, and X. Yu, "Polycaprolactone and bovine serum albumin based nanofibers for controlled release of nerve growth factor," *Biomacromolecules*, vol. 10, no. 5, pp. 1084–1089, 2009.

[9] L. Xiaoqiang, S. Yan, C. Rui et al., "Fabrication and properties of core-shell structure P(LLA-CL) nanofibers by coaxial electrospinning," *Journal of Applied Polymer Science*, vol. 111, no. 3, pp. 1564–1570, 2009.

[10] X. Xu, L. Yang, X. Xu et al., "Ultrafine medicated fibers electrospun from W/O emulsions," *Journal of Controlled Release*, vol. 108, no. 1, pp. 33–42, 2005.

[11] S. Yan, L. Xiaoqiang, T. Lianjiang, H. Chen, and M. Xiumei, "Poly(l-lactide-co-ε-caprolactone) electrospun nanofibers for encapsulating and sustained releasing proteins," *Polymer*, vol. 50, no. 17, pp. 4212–4219, 2009.

[12] Y. Z. Zhang, X. Wang, Y. Feng, J. Li, C. T. Lim, and S. Ramakrishna, "Coaxial electrospinning of (fluorescein isothiocyanate-conjugated bovine serum albumin)-encapsulated poly(ε-caprolactone) nanofibers for sustained release," *Biomacromolecules*, vol. 7, no. 4, pp. 1049–1057, 2006.

[13] E.-R. Kenawy, G. L. Bowlin, K. Mansfield et al., "Release of tetracycline hydrochloride from electrospun poly(ethylene-co-vinylacetate), poly(lactic acid), and a blend," *Journal of Controlled Release*, vol. 81, no. 1-2, pp. 57–64, 2002.

[14] G. Verreck, I. Chun, J. Rosenblatt et al., "Incorporation of drugs in an amorphous state into electrospun nanofibers composed of a water-insoluble, nonbiodegradable polymer," *Journal of Controlled Release*, vol. 92, no. 3, pp. 349–360, 2003.

[15] X. Zong, K. Kim, D. Fang, S. Ran, B. S. Hsiao, and B. Chu, "Structure and process relationship of electrospun bioabsorbable nanofiber membranes," *Polymer*, vol. 43, no. 16, pp. 4403–4412, 2002.

[16] H. Wang, Y. Feng, H. Zhao et al., "Controlled heparin release from electrospun gelatin fibers," *Journal of Controlled Release*, vol. 152, supplement 1, pp. e28–e29, 2011.

[17] Y. Su and X. Mo, "Dual drug release from coaxial electrospun nanofibers," *Journal of Controlled Release*, vol. 152, supplement 1, pp. e82–e84, 2011.

[18] E. Luong-Van, L. Grøndahl, K. N. Chua, K. W. Leong, V. Nurcombe, and S. M. Cool, "Controlled release of heparin from poly(ε-caprolactone) electrospun fibers," *Biomaterials*, vol. 27, no. 9, pp. 2042–2050, 2006.

[19] K. Kim, Y. K. Luu, C. Chang et al., "Incorporation and controlled release of a hydrophilic antibiotic using poly(lactide-co-glycolide)-based electrospun nanofibrous scaffolds," *Journal of Controlled Release*, vol. 98, no. 1, pp. 47–56, 2004.

[20] J. K. Tessmar and A. M. Göpferich, "Matrices and scaffolds for protein delivery in tissue engineering," *Advanced Drug Delivery Reviews*, vol. 59, no. 4-5, pp. 274–291, 2007.

[21] J. Zeng, L. Yang, Q. Liang et al., "Influence of the drug compatibility with polymer solution on the release kinetics of electrospun fiber formulation," *Journal of Controlled Release*, vol. 105, no. 1-2, pp. 43–51, 2005.

[22] C. K. S. Pillai, W. Paul, and C. P. Sharma, "Chitin and chitosan polymers: chemistry, solubility and fiber formation," *Progress in Polymer Science*, vol. 34, no. 7, pp. 641–678, 2009.

[23] M. Z. Elsabee, H. F. Naguib, and R. E. Morsi, "Chitosan based nanofibers, review," *Materials Science and Engineering C*, vol. 32, no. 7, pp. 1711–1726, 2012.

[24] K. Sun and Z. H. Li, "Preparations, properties and applications of chitosan based nanofibers fabricated by electrospinning," *Express Polymer Letters*, vol. 5, no. 4, pp. 342–361, 2011.

[25] X. Geng, O.-H. Kwon, and J. Jang, "Electrospinning of chitosan dissolved in concentrated acetic acid solution," *Biomaterials*, vol. 26, no. 27, pp. 5427–5432, 2005.

[26] K. Ohkawa, D. Cha, H. Kim, A. Nishida, and H. Yamamoto, "Electrospinning of chitosan," *Macromolecular Rapid Communications*, vol. 25, no. 18, pp. 1600–1605, 2004.

[27] H. Homayoni, S. A. H. Ravandi, and M. Valizadeh, "Electrospinning of chitosan nanofibers: processing optimization," *Carbohydrate Polymers*, vol. 77, no. 3, pp. 656–661, 2009.

[28] J. D. Schiffman and C. L. Schauer, "Cross-linking chitosan nanofibers," *Biomacromolecules*, vol. 8, no. 2, pp. 594–601, 2007.

[29] H. Homayoni, S. A. H. Ravandi, and M. Valizadeh, "Influence of the molecular weight of chitosan on the spinnability of chitosan/poly(vinyl alcohol) blend nanofibers," *Journal of Applied Polymer Science*, vol. 113, no. 4, pp. 2507–2513, 2009.

[30] F. Roozbahani, N. Sultana, A. Fauzi Ismail, and H. Nouparvar, "Effects of chitosan alkali pretreatment on the preparation of electrospun PCL/chitosan blend nanofibrous scaffolds for tissue engineering application," *Journal of Nanomaterials*, vol. 2013, Article ID 641502, 6 pages, 2013.

[31] K. T. Shalumon, K. H. Anulekha, K. P. Chennazhi, H. Tamura, S. V. Nair, and R. Jayakumar, "Fabrication of chitosan/poly(caprolactone) nanofibrous scaffold for bone and skin tissue engineering," *International Journal of Biological Macromolecules*, vol. 48, no. 4, pp. 571–576, 2011.

[32] S. Hong and G. Kim, "Fabrication of electrospun polycaprolactone biocomposites reinforced with chitosan for the proliferation of mesenchymal stem cells," *Carbohydrate Polymers*, vol. 83, no. 2, pp. 940–946, 2011.

[33] A. Cooper, N. Bhattarai, and M. Zhang, "Fabrication and cellular compatibility of aligned chitosan-PCL fibers for nerve tissue regeneration," *Carbohydrate Polymers*, vol. 85, no. 1, pp. 149–156, 2011.

[34] Y. Zhang, H. Ouyang, T. L. Chwee, S. Ramakrishna, and Z.-M. Huang, "Electrospinning of gelatin fibers and gelatin/PCL composite fibrous scaffolds," *Journal of Biomedical Materials Research Part B: Applied Biomaterials*, vol. 72, no. 1, pp. 156–165, 2005.

[35] E. J. Chong, T. T. Phan, I. J. Lim et al., "Evaluation of electrospun PCL/gelatin nanofibrous scaffold for wound healing and layered dermal reconstitution," *Acta Biomaterialia*, vol. 3, no. 3, pp. 321–330, 2007.

[36] L. van der Schueren, I. Steyaert, B. de Schoenmaker, and K. de Clerck, "Polycaprolactone/chitosan blend nanofibres electrospun from an acetic acid/formic acid solvent system," *Carbohydrate Polymers*, vol. 88, no. 4, pp. 1221–1226, 2012.

[37] X. Yang, X. Chen, and H. Wang, "Acceleration of osteogenic differentiation of preosteoblastic cells by chitosan containing nanofibrous scaffolds," *Biomacromolecules*, vol. 10, no. 10, pp. 2772–2778, 2009.

[38] L. van der Schueren, B. de Schoenmaker, Ö. I. Kalaoglu, and K. de Clerck, "An alternative solvent system for the steady state electrospinning of polycaprolactone," *European Polymer Journal*, vol. 47, no. 6, pp. 1256–1263, 2011.

[39] D. H. Reneker and A. L. Yarin, "Electrospinning jets and polymer nanofibers," *Polymer*, vol. 49, no. 10, pp. 2387–2425, 2008.

[40] H. Qi, P. Hu, J. Xu, and A. Wang, "Encapsulation of drug reservoirs in fibers by emulsion electrospinning: morphology characterization and preliminary release assessment," *Biomacromolecules*, vol. 7, no. 8, pp. 2327–2330, 2006.